Capacity of Rayleigh Fading Channels Under Different Adaptive Transmission and Diversity-Combining Techniques

Mohamed-Slim Alouini, *Member IEEE,* and Andrea J. Goldsmith, *Member, IEEE*

Abstract— We study the Shannon capacity of adaptive transmission techniques in conjunction with diversity combining. This capacity provides an upper bound on spectral efficiency using these techniques. We obtain closed-form solutions for the Rayleigh fading channel capacity under three adaptive policies: optimal power and rate adaptation, constant power with optimal rate adaptation, and channel inversion with fixed rate. Optimal power and rate adaptation yields a small increase in capacity over just rate adaptation, and this increase diminishes as the average received carrier-to-noise ratio (CNR) or the number of diversity branches increases. Channel inversion suffers the largest capacity penalty relative to the optimal technique, however, the penalty diminishes with increased diversity. Although diversity yields large capacity gains for all the techniques, the gain is most pronounced with channel inversion. For example, the capacity using channel inversion with two-branch diversity exceeds that of a single-branch system using optimal rate and power adaptation. Since channel inversion is the least complex scheme to implement, there is a tradeoff between complexity and capacity for the various adaptation methods and diversity-combining techniques.

Index Terms— Adaptive transmission techniques, diversity combining, Shannon capacity.

I. INTRODUCTION

THE RADIO spectrum available for wireless services is extremely scarce, while demand for these service is growing at a rapid pace [1]. Spectral efficiency is therefore of primary concern in the design of future wireless data communications systems. High overall spectral efficiency of a wireless cellular system may be achieved at several levels of the system design [2]:

- at the radio coverage planning level by minimizing cell area and the cochannel reuse distance;
- at the network/system level by using sophisticated channel allocation schemes that maximize the overall carried traffic;
- at the communication link level through a skillful combination of bandwidth efficient coding and modulation techniques.

In this paper, we focus on the link spectral efficiency, defined as the average transmitted data rate per unit bandwidth for a specified average transmit power and bit error rate (BER). Over the last three decades, researchers have looked at various ways to improve the link spectral efficiency of wireless systems. In what follows, we first briefly summarize the major steps and progress achieved in that arena. We then present the objectives and outline of our paper.

A. Spectral Efficiency over Fading Channels

Multilevel modulation schemes, such as MQAM, increase link spectral efficiency by sending multiple bits per symbol [3]. Unfortunately, mobile radio links are subject to severe multipath fading due to the combination of randomly delayed reflected, scattered, and diffracted signal components [4]. Fading leads to serious degradation in the link carrier-to-noise ratio (CNR), resulting in either a higher BER or a higher required transmit power for a given multilevel modulation technique. Thus, fading compensation is typically required to improve link performance. One compensation technique, proposed by Sampei and Sunaga [5], uses pilot symbol-assisted modulation (PSAM). This technique inserts a training sequence into the stream of MQAM data symbols to extract the channel-induced attenuation and phase shift, which are then used for symbol detection. Space diversity, which combines signals received over several antenna branches, is another powerful technique to combat fading [6]. Diversity can often be combined with other fading compensation methods to mitigate most of the fading degradation. For example, joint use of PSAM and maximal ratio combining (MRC) antenna diversity was proposed in [7], and field trials with this technique demonstrated considerable performance improvement over MQAM without compensation [8], [9].

Other fading compensation techniques include an increased link budget margin or interleaving with channel coding [2]. However, these techniques are designed relative to the worst case channel conditions, resulting in poor utilization of the full channel capacity a good percentage of the time (under negligible or shallow fading conditions). Adapting certain parameters of the transmitted signal to the channel fading leads to better utilization of the channel capacity. The concept
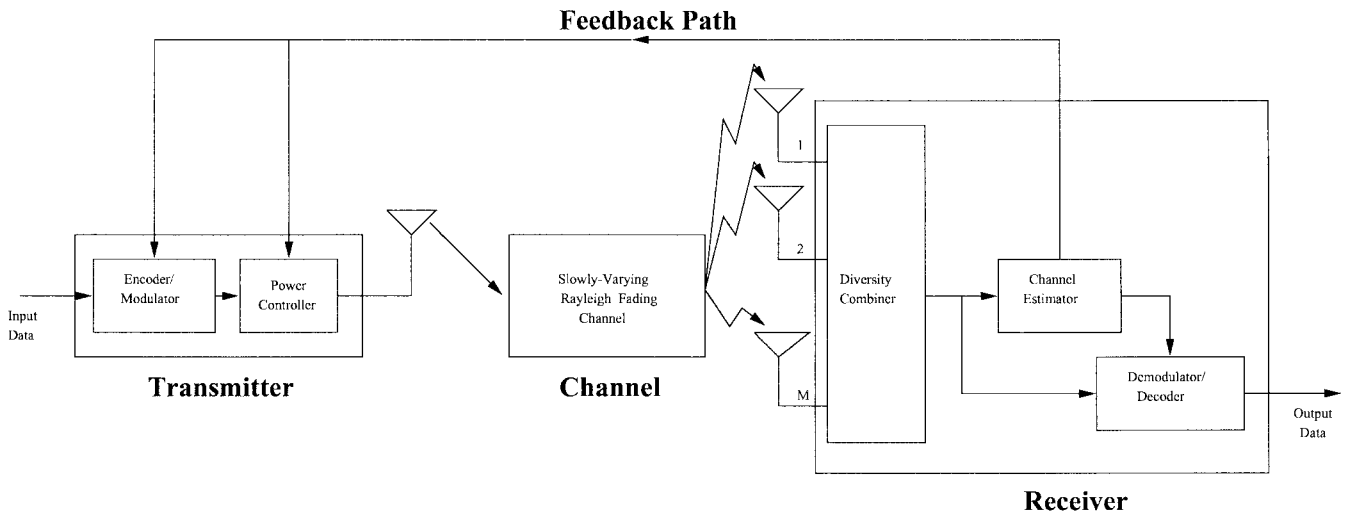
Feedback Path

Fig. 1.   Transmission system block diagram.

of adaptive transmission, which requires accurate channel estimation at the receiver and a reliable feedback path between that estimator and the transmitter, was first proposed around the late 1960's [10]–[12]. Interest in these techniques was short lived, perhaps due to hardware constraints, lack of good channel estimation techniques, and/or systems focusing on point-to-point radio links without transmitter feedback. The fact that these issues are less constraining in current land mobile radio systems, coupled with the need for spectrally efficient communication, has revived interest in adaptive modulation methods. The main idea behind these schemes is real-time balancing of the link budget through adaptive variation of the transmitted power level [10], symbol rate [11], constellation size [13]–[15], coding rate/scheme [16], or any combination of these parameters [12], [17]–[22]. Thus, without sacrificing BER these schemes provide a much higher average spectral efficiency by taking advantage of the "time-varying" nature of the wireless channel: transmitting at high speeds under favorable channel conditions and responding to channel degradation through a smooth reduction of their data throughput. The performance of these schemes is further improved by combining them with space diversity [23]. The disadvantage of these adaptive techniques is that they require an accurate channel estimate at the transmitter, additional hardware complexity to implement adaptive transmission, and buffering/delay of the input data since the transmission rate varies with channel conditions.

B. Objective and Outline

The aim of this paper is to investigate the theoretical spectral efficiency limits of adaptive modulation in Rayleigh fading channels. This fading channel model applies to land mobile radio channels without a line-of-sight path between the transmitter and receiver antennas, as well as to ionospheric [24] and tropospheric scatter [25] channels. Our analyses can also be generalized to Nakagami fading channels [26].

The Shannon capacity of a channel defines its theoretical upper bound for the maximum rate of data transmission at an arbitrarily small BER, without any delay or complex-

ity constraints. Therefore, the Shannon capacity represents an optimistic bound for practical communication schemes, and also serves as a benchmark against which to compare the spectral efficiency of all practical adaptive transmission schemes [19]. In [27], the capacity of a single-user flat-fading channel with channel measurement information at the transmitter and receiver was derived for various adaptive transmission policies. In this paper, we apply the general theory developed in [27] to obtain closed-form expressions for the capacity of Rayleigh fading channels under different adaptive transmission and diversity-combining techniques. In particular, we consider three adaptation policies: optimal simultaneous power and rate adaptation, constant power with optimal rate adaptation, and channel inversion with fixed rate. We investigate the relative impact of MRC and selective combining (SC) diversity schemes in conjunction with each of these adaptive transmission schemes. Note that an analytical evaluation of the capacity in a Rayleigh fading environment with the constant power policy was carried out in [28]–[30]. We extend this analysis to derive closed-from expressions for capacity with MRC and SC and compare it to the capacity of the other adaptive methods.

The remainder of this paper is organized as follows. In Section II, we outline the channel and communication system model. We derive the capacity of a Rayleigh fading channel (with and without diversity) for the optimal adaptation policy, constant power policy, and channel inversion policy in Sections III–V, respectively. In Section VI, we present some numerical examples comparing: 1) the Rayleigh channel capacity with the capacity of an additive white Gaussian noise (AWGN) channel and 2) the Rayleigh channel capacity for the various adaptation policies and diversity-combining techniques under consideration. We review our main results and offer some concluding remarks in Section VII.

II. CHANNEL AND SYSTEM MODEL

In this section, we describe the channel and communication system model. A block diagram of the transmission system is shown in Fig. 1.

We assume that the channel changes at a rate much slower than the data rate, so the channel remains constant over hundreds of symbols. We call this a slowly varying channel. We assume a Rayleigh fading channel so that the probability distribution function (PDF) of CNR (γ) is given by an exponential distribution [4, eq. (5.2-13), p. 314]

$$p_\gamma(\gamma) = \frac{e^{-\gamma/\overline{\gamma}}}{\overline{\gamma}}, \qquad \gamma \geq 0 \tag{1}$$

where $\overline{\gamma}$ is the average received CNR.

We consider both MRC and SC diversity combining of the received signal. MRC diversity combining requires that the individual signals from each branch be weighted by their signal voltage to noise power ratios then summed coherently [4, p. 316]. In our MRC analyses, we assume perfect knowledge of the branch amplitudes and phases, which we call *perfect combining*. MRC with perfect combining is the optimal diversity scheme [4, p. 316] and therefore provides the maximum capacity improvement relative to all combining techniques. The disadvantage of MRC is that it requires knowledge of the branch parameters and independent processing of each branch. Let $\overline{\gamma}_k$ denote the average CNR on the kth branch. For independent branch signals and equal average branch CNR $\overline{\gamma}$

$$\overline{\gamma}_k = \overline{\gamma}, \qquad \text{for all} \quad k \in \{1, 2, 3, \cdots, M\} \tag{2}$$

the PDF of the received CNR at the output of a perfect M-branch MRC combiner is a chi-square distribution with $2M$ degrees of freedom [4, eq. (5.2-14), p. 319] given by

$$p_\gamma^{\text{mrc}}(\gamma) = \frac{\gamma^{M-1} e^{-\gamma/\overline{\gamma}}}{(M-1)! \overline{\gamma}^M}, \qquad \gamma \geq 0. \tag{3}$$

SC diversity only processes one of the diversity branches. Specifically, the combiner chooses the branch with the highest CNR [4, p. 313]. Thus, this diversity-combining technique is simpler than MRC, but also yields suboptimal performance. Since the output of the SC combiner is equal to the signal on one of the branches, the coherent sum of the individual branch signals is not required.[1] Assuming independent branch signals and equal average branch CNR (2), the PDF of the received CNR at the output of an M-branch SC combiner is given by [4, eq. (5.2-7), p. 316]

$$p_\gamma^{\text{sc}}(\gamma) = \frac{M}{\overline{\gamma}} (1 - e^{-\gamma/\overline{\gamma}})^{M-1} e^{-\gamma/\overline{\gamma}}, \qquad \gamma \geq 0. \tag{4}$$

Note that using the binomial expansion, we can rewrite (4) as

$$p_\gamma^{\text{sc}}(\gamma) = \frac{M}{\overline{\gamma}} \sum_{k=0}^{M-1} (-1)^k \binom{M-1}{k} e^{-(1+k)\gamma/\overline{\gamma}} \tag{5}$$

where $\binom{M-1}{k}$ denotes the binomial coefficient given by

$$\binom{M-1}{k} = \frac{(M-1)!}{(M-k-1)! k!}. \tag{6}$$

We assume throughout our analyses that the variation in the combiner output CNR γ is tracked perfectly by the receiver.

---

[1] The SC scheme can therefore be used in conjunction with differential modulation techniques, in contrast to MRC, which is restricted by design to coherent modulations.

We also assume that the variation in γ is sent back to the transmitter via an error-free feedback path. The time delay in this feedback path is assumed to be negligible compared to the rate of the channel variation. All these assumptions, which are reasonable for high-speed data transmission over a slowly fading channel, allow the transmitter to adapt its power and/or rate relative to the actual channel state.

III. OPTIMAL SIMULTANEOUS POWER AND RATE ADAPTATION

Given an average transmit power constraint, the channel capacity of a fading channel with received CNR distribution $p_\gamma(\gamma)$ and optimal power and rate adaptation ($\langle C \rangle_{\text{opra}}$ [b/s]) is given in [27] as

$$\langle C \rangle_{\text{opra}} = B \int_{\gamma_o}^{+\infty} \log_2 \left(\frac{\gamma}{\gamma_o} \right) p_\gamma(\gamma) \, d\gamma \tag{7}$$

where B [Hz] is the channel bandwidth and γ_o is the optimal cutoff CNR level below which data transmission is suspended. This optimal cutoff must satisfy

$$\int_{\gamma_o}^{+\infty} \left(\frac{1}{\gamma_o} - \frac{1}{\gamma} \right) p_\gamma(\gamma) \, d\gamma = 1. \tag{8}$$

To achieve the capacity (7), the channel fade level must be tracked at both the receiver and transmitter, and the transmitter has to adapt its power and rate accordingly, allocating high-power levels and rates for good channel conditions (γ large), and lower power levels and rates for unfavorable channel conditions (γ small). Since no data is sent when $\gamma < \gamma_o$, the optimal policy suffers a probability of outage P_{out}, equal to the probability of no transmission, given by

$$P_{\text{out}} = P[\gamma \leq \gamma_o] = \int_0^{\gamma_o} p_\gamma(\gamma) \, d\gamma$$
$$= 1 - \int_{\gamma_o}^{+\infty} p_\gamma(\gamma) \, d\gamma. \tag{9}$$

We now obtain closed-form expressions for the optimal cutoff CNR γ_o, capacity $\langle C \rangle_{\text{opra}}$, and outage probability P_{out} of this optimal adaptation technique with and without diversity combining. No numerical integrations are required, though numerical root finding is needed to find γ_o.

A. No Diversity

Substituting (1) in (8) we find that γ_o must satisfy

$$E_0 \left(\frac{\gamma_o}{\overline{\gamma}} \right) - E_1 \left(\frac{\gamma_o}{\overline{\gamma}} \right) = \overline{\gamma} \tag{10}$$

where $E_n(x)$ is the exponential integral of order n defined by

$$E_n(x) = \int_1^{+\infty} t^{-n} e^{-xt} \, dt, \qquad x \geq 0. \tag{11}$$

In particular, $E_0(x) = e^{-x}/x$ so (10) reduces to

$$\frac{e^{-\gamma_o/\overline{\gamma}}}{\gamma_o/\overline{\gamma}} - E_1 \left(\frac{\gamma_o}{\overline{\gamma}} \right) = \overline{\gamma}. \tag{12}$$

Let $x = \gamma_o/\overline{\gamma}$ and define

$$f(x) = \frac{e^{-x}}{x} - E_1(x) - \overline{\gamma}. \tag{13}$$

Note that $(df(x)/dx) = (-e^{-x}/x^2) < 0$ for all $x \geq 0$. Moreover, from (13), $\lim_{x \to 0^+} f(x) = +\infty$ and $\lim_{x \to +\infty} f(x) = -\overline{\gamma} < 0$. Thus, we conclude that there is a unique x_o for which $f(x_o) = 0$ or, equivalently, there is a unique γ_o which satisfies (12). An asymptotic expansion of (12) shows that as $\overline{\gamma} \to +\infty$, $\gamma_o \to 1$. Our numerical results show that γ_o increases as $\overline{\gamma}$ increases, so γ_o always lies in the interval $[0, 1]$.

Substituting (1) in (7), and defining the integral $\mathcal{J}_n(\mu)$ as

$$\mathcal{J}_n(\mu) = \int_1^{+\infty} t^{n-1} \ln t e^{-\mu t} \, dt,$$
$$\mu > 0; n = 1, 2, \cdots \tag{14}$$

we can rewrite the channel capacity $\langle C \rangle_{\text{opra}}$ as

$$\langle C \rangle_{\text{opra}} = B \log_2(e) \frac{\gamma_o}{\overline{\gamma}} \mathcal{J}_1\left(\frac{\gamma_o}{\overline{\gamma}}\right). \tag{15}$$

The evaluation of $\mathcal{J}_1(\mu)$ is derived in the Appendix A and given in (71). Using that result we obtain the capacity per unit bandwidth $\langle C \rangle_{\text{opra}}/B$ [b/s/Hz] as

$$\frac{\langle C \rangle_{\text{opra}}}{B} = \log_2(e) E_1\left(\frac{\gamma_o}{\overline{\gamma}}\right). \tag{16}$$

Using (12) in (16), the optimal capacity per unit bandwidth reduces to the simple expression

$$\frac{\langle C \rangle_{\text{opra}}}{B} = \log_2(e)\left(\frac{e^{-\gamma_o/\overline{\gamma}}}{\gamma_o/\overline{\gamma}} - \overline{\gamma}\right). \tag{17}$$

Using (1) in the probability of outage (9) yields

$$P_{\text{out}} = 1 - e^{-\gamma_o/\overline{\gamma}}. \tag{18}$$

B. Maximal Ratio Combining

Inserting the CNR distribution (3) in (8) we see that with MRC combining γ_o must satisfy

$$\frac{\Gamma\left(M, \frac{\gamma_o}{\overline{\gamma}}\right)}{\frac{\gamma_o}{\overline{\gamma}}} - \Gamma\left(M-1, \frac{\gamma_o}{\overline{\gamma}}\right) = (M-1)!\overline{\gamma} \tag{19}$$

where $\Gamma(\cdot, \cdot)$ is the complementary incomplete gamma function defined in (65). Let $x = \gamma_o/\overline{\gamma}$ and define

$$f_{\text{mrc}}(x) = \frac{\Gamma(M, x)}{x} - \Gamma(M-1, x) - (M-1)!\overline{\gamma}. \tag{20}$$

Note that $(df_{\text{mrc}}(x)/dx) = (-\Gamma(M, x)/x^2) < 0$ for all $x \geq 0$ and $M \geq 2$. Since $\lim_{x \to 0^+} f_{\text{mrc}}(x) = +\infty$ and $\lim_{x \to +\infty} f_{\text{mrc}}(x) = -(M-1)!\overline{\gamma} < 0$, we conclude that there is a unique x_o such that $f_{\text{mrc}}(x_o) = 0$ or, equivalently, there is a unique γ_o which satisfies (19). An asymptotic expansion on (19) shows that $\gamma_o \to 1$ as $\overline{\gamma} \to +\infty$, so $\gamma_o \in [0, 1]$. Comparing this with the results in Section III-A, we see that as the average received CNR grows to infinity, the optimal cutoff value is unaffected by diversity.

Substituting (3) in (7) we obtain the channel capacity with MRC diversity, $\langle C \rangle_{\text{opra}}^{\text{mrc}}$ [b/s], in terms of the integral $\mathcal{J}_M(\cdot)$ as

$$\langle C \rangle_{\text{opra}}^{\text{mrc}} = \frac{B \log_2(e)}{(M-1)!}\left(\frac{\gamma_o}{\overline{\gamma}}\right)^M \mathcal{J}_M\left(\frac{\gamma_o}{\overline{\gamma}}\right). \tag{21}$$

The evaluation of $\mathcal{J}_n(\mu)$ is derived in the Appendix A and given in (70). Using that result, we obtain the capacity per unit bandwidth $\langle C \rangle_{\text{opra}}^{\text{mrc}}/B$ [b/s/Hz] as

$$\frac{\langle C \rangle_{\text{opra}}^{\text{mrc}}}{B} = \log_2(e)\left(E_1(\gamma_o/\overline{\gamma}) + \sum_{k=1}^{M-1} \frac{\mathcal{P}_k(\gamma_o/\overline{\gamma})}{k}\right) \tag{22}$$

where $\mathcal{P}_k(\cdot)$ denotes the Poisson distribution defined in (67). The corresponding probability of outage $P_{\text{out}}^{\text{mrc}}$ is obtained by substituting (3) into (9), and using [31, eq. (8.381.3), p. 364] and (66)

$$P_{\text{out}}^{\text{mrc}} = 1 - \mathcal{P}_M(\gamma_o/\overline{\gamma}). \tag{23}$$

C. Selection Combining

Substituting the CNR distribution (5) into (8) we find that γ_o must satisfy

$$\sum_{k=0}^{M-1} (-1)^k \binom{M-1}{k}\left(\frac{e^{-(1+k)\gamma_o/\overline{\gamma}}}{(1+k)\gamma_o/\overline{\gamma}} - E_1((1+k)\gamma_o/\overline{\gamma})\right)$$
$$= \overline{\gamma}/M. \tag{24}$$

Let $x = \gamma_o/\overline{\gamma}$ and define

$$f_{\text{sc}}(x) = \sum_{k=0}^{M-1} (-1)^k \binom{M-1}{k}\left(\frac{e^{-(1+k)x}}{(1+k)x} - E_1((1+k)x)\right)$$
$$- \overline{\gamma}/M. \tag{25}$$

Note that $(df_{\text{sc}}(x)/dx) = -\Sigma_{k=0}^{M-1} a_k(x)$, where $a_k(x) = (-1)^k \binom{M-1}{k}(e^{-(1+k)x}/(1+k)^2 x^2)$. Since $a_0(x) = e^{-x}/x^2 > 0$ and, for all $k \leq M$, $|a_{k+1}(x)| < |a_k(x)|$, we have $(df_{\text{sc}}(x)/dx) < 0$ for all $x \geq 0$. Moreover, from (25), $\lim_{x \to 0^+} f_{\text{sc}}(x) = +\infty$ and $\lim_{x \to +\infty} f_{\text{sc}}(x) = -\overline{\gamma}/M < 0$. Thus, we conclude that there is a unique x_o for which $f_{\text{sc}}(x_o) = 0$ or, equivalently, there is a unique γ_o which satisfies (24). An asymptotic expansion of (24) shows that as $\overline{\gamma} \to +\infty$, $\gamma_o \to 1$. Therefore, as in the no diversity and MRC diversity cases, γ_o always lies in the interval $[0, 1]$.

Inserting (5) into (7), we can express the channel capacity with SC diversity, $\langle C \rangle_{\text{opra}}^{\text{sc}}$ [b/s], in terms of the integral $\mathcal{J}_1(\cdot)$ as

$$\langle C \rangle_{\text{opra}}^{\text{sc}} = BM \log_2(e) \frac{\gamma_o}{\overline{\gamma}} \sum_{k=0}^{M-1} (-1)^k \binom{M-1}{k}$$
$$\cdot \mathcal{J}_1\left(\frac{(1+k)\gamma_o}{\overline{\gamma}}\right). \tag{26}$$

Using (71) from Appendix A, we obtain the capacity per unit bandwidth, $\langle C \rangle_{\text{opra}}^{\text{sc}}/B$ [b/s/Hz], as

$$\frac{\langle C \rangle_{\text{opra}}^{\text{sc}}}{B} = M \log_2(e) \sum_{k=0}^{M-1} (-1)^k \binom{M-1}{k}$$
$$\cdot \frac{E_1((1+k)\gamma_o/\overline{\gamma})}{1+k}. \tag{27}$$

The corresponding probability of outage $P_{\text{out}}^{\text{sc}}$ is obtained by substituting (5) into (9)

$$P_{\text{out}}^{\text{sc}} = 1 - M \sum_{k=0}^{M-1} (-1)^k \binom{M-1}{k} \frac{e^{-(1+k)\gamma_o/\overline{\gamma}}}{1+k}. \quad (28)$$

We see from (28) that as $\overline{\gamma}$ tends to infinity (and γ_o tends to one) $P_{\text{out}}^{\text{sc}}$ tends to zero, as expected. Similarly, we can also see from (28) that as γ_o tends to zero (i.e., total channel inversion) $P_{\text{out}}^{\text{sc}}$ tends to zero.

IV. OPTIMAL RATE ADAPTATION WITH CONSTANT TRANSMIT POWER

With optimal rate adaptation to channel fading with a constant transmit power, the channel capacity $\langle C \rangle_{\text{ora}}$ [b/s] becomes [27], [32]

$$\langle C \rangle_{\text{ora}} = B \int_0^{+\infty} \log_2 (1+\gamma) p_\gamma(\gamma) \, d\gamma. \quad (29)$$

$\langle C \rangle_{\text{ora}}$ was previously introduced by Lee [28] as the average channel capacity of a flat-fading channel, since it is obtained by averaging the capacity of an AWGN channel

$$C_{\text{awgn}} = B \log_2 (1+\gamma) \quad (30)$$

over the distribution of the received CNR γ. In fact, (29) represents the capacity of the fading channel without transmitter feedback (i.e., with the channel fade level known at the receiver only) [29], [33], [34]. In the following analysis, we first obtain the channel capacity without diversity (correcting some minor errors in [28]) and then derive analytical expressions as well as simple accurate asymptotic approximations of the capacity improvement with both MRC and SC diversity.

A. No Diversity

Substituting (1) into (29), the channel capacity $\langle C \rangle_{\text{ora}}$ of a Rayleigh fading channel is obtained as

$$\langle C \rangle_{\text{ora}} = \int_0^{+\infty} B \log_2 (1+\gamma) \frac{e^{-\gamma/\overline{\gamma}}}{\overline{\gamma}} \, d\gamma. \quad (31)$$

Defining the integral $\mathcal{I}_n(\mu)$ as

$$\mathcal{I}_n(\mu) = \int_0^{+\infty} t^{n-1} \ln (1+t) e^{-\mu t} \, dt;$$
$$\mu > 0; n = 1, 2, \cdots \quad (32)$$

we can rewrite $\langle C \rangle_{\text{ora}}$ as

$$\langle C \rangle_{\text{ora}} = B \log_2 (e) \frac{\mathcal{I}_1(1/\overline{\gamma})}{\overline{\gamma}}. \quad (33)$$

Using the result of (80) from the Appendix B, we can write $\langle C \rangle_{\text{ora}}/B$ [b/s/Hz] as

$$\frac{\langle C \rangle_{\text{ora}}}{B} = \log_2 (e) e^{1/\overline{\gamma}} E_1(1/\overline{\gamma}). \quad (34)$$

Note that the exponential-integral function of first order, $E_1(\cdot)$, is related to the exponential-integral function, $E_i(\cdot)$, used in [28] by $E_1(x) = -E_i(-x)$.

Using the first series expansion for $E_1(\cdot)$ [28, eq. (6)], and substituting it into (34) yields

$$\frac{\langle C \rangle_{\text{ora}}}{B} = \log_2 (e) e^{1/\overline{\gamma}} \left(-E + \ln \overline{\gamma} - \sum_{k=1}^{+\infty} \frac{(-1/\overline{\gamma})^k}{k \cdot k!} \right) \quad (35)$$

where E is the Euler constant ($E = 0.577\,215\,665$). Therefore, for $\overline{\gamma} \gg 1$, we get the following approximation for (34):

$$\frac{\langle C \rangle_{\text{ora}}}{B} \simeq \log_2 (e) e^{1/\overline{\gamma}} \left(-E + \ln \overline{\gamma} + \frac{1}{\overline{\gamma}} \right). \quad (36)$$

Using the second series expansion for $E_1(\cdot)$ given by [28, eq. (7)] and substituting it in (34) yields

$$\langle C \rangle_{\text{ora}} = B \log_2 (e) \sum_{k=1}^{n} (-1)^{(k+1)} (k-1)! \overline{\gamma}^k + R_n \quad (37)$$

where R_n is a remainder term. Taking the limit as the channel bandwidth approaches infinity yields

$$\lim_{B \to +\infty} \langle C \rangle_{\text{ora}} = \log_2 (e) \frac{\langle S \rangle}{N_o} \quad (38)$$

where $\langle S \rangle$ [W] is the average carrier power and N_o [W/Hz] is the noise density power per unit bandwidth.[2]

B. Maximal Ratio Combining

Substituting (3) into (29), we obtain the channel capacity $\langle C \rangle_{\text{ora}}^{\text{mrc}}$ [b/s] with MRC in terms of the integral $\mathcal{I}_M(\cdot)$ as

$$\langle C \rangle_{\text{ora}}^{\text{mrc}} = B \log_2 (e) \frac{\mathcal{I}_M(1/\overline{\gamma})}{(M-1)! \overline{\gamma}^M}. \quad (39)$$

Using (78) from Appendix B, we can rewrite $\langle C \rangle_{\text{ora}}^{\text{mrc}}/B$ [b/s/Hz] as

$$\frac{\langle C \rangle_{\text{ora}}^{\text{mrc}}}{B} = \log_2 (e) e^{1/\overline{\gamma}} \sum_{k=0}^{M-1} \frac{\Gamma(-k, 1/\overline{\gamma})}{\overline{\gamma}^k} \quad (40)$$

where $\Gamma(\cdot, \cdot)$ is the complementary incomplete gamma function defined in (65). Note that by using [31, eq. (8.359.1), p. 951], the capacity with the MRC diversity scheme (40) with a single branch ($M = 1$) reduces to (34), as expected. Note also that by using [31, eq. (8.352.3), p. 950] and [31, eq. (8.359.1), p. 951], one may express (40) in terms of the Poisson distribution as [30, eq. (7)]

$$\frac{\langle C \rangle_{\text{ora}}^{\text{mrc}}}{B} = \log_2 (e) \left(\mathcal{P}_M(-1/\overline{\gamma}) E_1(1/\overline{\gamma}) \right.$$
$$\left. + \sum_{k=1}^{M-1} \frac{\mathcal{P}_k(1/\overline{\gamma}) \mathcal{P}_{M-k}(-1/\overline{\gamma})}{k} \right). \quad (41)$$

---

[2] In [28], the average CNR $\overline{\gamma}$ is denoted by Γ. Note the typographical error in [28, eq. (4)] (γ instead of Γ in the denominator) and the resulting sign difference in the argument of the exponential term $e^{1/\overline{\gamma}}$ between our result (34) and [28, eq. (5)] and between (36) and [28, eq. (9)]. There is also a sign difference between (37) and [28, eq. (10)]. However, the limit (38) matches the limiting expression [28, eq. (11)], so the sign error in [28, eq. (10)] was corrected in the limit.

Moreover, using the first series expansion for $E_1(\cdot)$ [28, eq. (6)] in (41) we obtain an asymptotic approximation $(\overline{\gamma} \gg 1)$ for $\langle C \rangle_{\mathrm{ora}}^{\mathrm{mrc}}/B$ as

$$\frac{\langle C \rangle_{\mathrm{ora}}^{\mathrm{mrc}}}{B} \simeq \log_2(e) \left(\mathcal{P}_M(-1/\overline{\gamma}) \left(-E + \ln \overline{\gamma} + \frac{1}{\overline{\gamma}} \right) + \sum_{k=1}^{M-1} \frac{\mathcal{P}_k(1/\overline{\gamma}) \mathcal{P}_{M-k}(-1/\overline{\gamma})}{k} \right). \tag{42}$$

Fig. 5 compares plots of (40) with its asymptotic approximation (42) and the results are discussed in Section VI-A.

C. Selection Combining

Substituting (5) into (29), we obtain the channel capacity $\langle C \rangle_{\mathrm{ora}}^{\mathrm{sc}}$ [b/s] with SC in terms of the integral $\mathcal{I}_1(\cdot)$ as

$$\langle C \rangle_{\mathrm{ora}}^{\mathrm{sc}} = \frac{BM}{\overline{\gamma}} \log_2(e) \sum_{k=0}^{M-1} (-1)^k \binom{M-1}{k} \cdot \mathcal{I}_1\left(\frac{1+k}{\overline{\gamma}} \right). \tag{43}$$

Then, using (80) from Appendix B, we can write $\langle C \rangle_{\mathrm{ora}}^{\mathrm{sc}}/B$ [b/s/Hz] as

$$\frac{\langle C \rangle_{\mathrm{ora}}^{\mathrm{sc}}}{B} = M \log_2(e) \sum_{k=0}^{M-1} (-1)^k \binom{M-1}{k} \cdot e^{(k+1)/\overline{\gamma}} \frac{E_1((1+k)/\overline{\gamma})}{1+k}. \tag{44}$$

We again note that for a single branch $(M = 1)$, (44) reduces to (34) as expected.

Using the first series expansion for $E_1(\cdot)$ [28, eq. (6)] and substituting it into (44) yields a simple asymptotic approximation $(\overline{\gamma} \gg 1)$ for $\langle C \rangle_{\mathrm{ora}}^{\mathrm{sc}}/B$ given by

$$\frac{\langle C \rangle_{\mathrm{ora}}^{\mathrm{sc}}}{B} \simeq M \log_2(e) \sum_{k=0}^{M-1} \frac{(-1)^{k+1}}{1+k} \binom{M-1}{k} \cdot e^{(1+k)/\overline{\gamma}} \left[E + \ln\left(\frac{1+k}{\overline{\gamma}} \right) - \left(\frac{1+k}{\overline{\gamma}} \right) \right]. \tag{45}$$

Fig. 6 compares plots of (44) with its asymptotic approximation (45) and the results are discussed in Section VI-A.

V. CHANNEL INVERSION WITH FIXED RATE

The channel capacity when the transmitter adapts its power to maintain a constant CNR at the receiver (i.e., inverts the channel fading) was also investigated in [27]. This technique uses fixed-rate modulation and a fixed code design, since the channel after channel inversion appears as a time-invariant AWGN channel. As a result, channel inversion with fixed rate is the least complex technique to implement, assuming good channel estimates are available at the transmitter and receiver. The channel capacity with this technique ($\langle C \rangle_{\mathrm{cifr}}$ [b/s]) is derived from the capacity of an AWGN channel and

is given in [27] as

$$\langle C \rangle_{\mathrm{cifr}} = B \log_2 \left(1 + \frac{1}{\int_0^{+\infty} p_\gamma(\gamma)/\gamma \, d\gamma} \right). \tag{46}$$

Channel inversion with fixed rate suffers a large capacity penalty relative to the other techniques, since a large amount of the transmitted power is required to compensate for the deep channel fades. A better approach is to use a modified inversion policy which inverts the channel fading only above a fixed cutoff fade depth γ_o. The capacity with this truncated channel inversion and fixed rate policy ($\langle C \rangle_{\mathrm{tifr}}$ [b/s]) was derived in [27] to be

$$\langle C \rangle_{\mathrm{tifr}} = B \log_2 \left(1 + \frac{1}{\int_{\gamma_o}^{+\infty} p_\gamma(\gamma)/\gamma \, d\gamma} \right) (1 - P_{\mathrm{out}}) \tag{47}$$

where P_{out} is given by (9). The cutoff level γ_o can be selected to achieve a specified outage probability or, alternatively, to maximize (47). The choice of γ_o is examined in more detail in the following sections.

We now derive closed-form expressions for the capacity under channel inversion with the different diversity combining techniques.

A. No Diversity

By substituting the CNR distribution (1) in (46) we find that the capacity of a Rayleigh fading channel with total channel inversion $\langle C \rangle_{\mathrm{cifr}}$ is zero. However, with truncated channel inversion the capacity per unit bandwidth $\langle C \rangle_{\mathrm{tifr}}/B$ [b/s/Hz] can be expressed in terms of $\overline{\gamma}$ and γ_o as

$$\frac{\langle C \rangle_{\mathrm{tifr}}}{B} = \log_2 \left(1 + \frac{\overline{\gamma}}{E_1(\gamma_o/\overline{\gamma})} \right) e^{-\gamma_o/\overline{\gamma}}. \tag{48}$$

Fig. 2 shows the dependence of $\langle C \rangle_{\mathrm{tifr}}/B$ on γ_o for different $\overline{\gamma}$ values. All these curves show that capacity is maximized for an optimal cutoff CNR γ_o^* which increases as a function of $\overline{\gamma}$. Recall that we proved the existence of a unique optimal cutoff CNR for the optimal adaptation policy in Section III-A. However, for optimal adaptation the optimal cutoff CNR γ_o was always bounded between [0, 1] (i.e., smaller than 0 dB), whereas for this policy γ_o^* is bigger than 0 dB when $\overline{\gamma} > 5$ dB. This means that for a fixed $\overline{\gamma}$, truncated channel inversion has both a smaller capacity (see Fig. 9) and a higher probability of outage (see Fig. 10) than the optimal policy of Section III.

B. Maximal Ratio Combining

We obtain the capacity per unit bandwidth for total channel inversion with MRC diversity combining, $\langle C \rangle_{\mathrm{cifr}}^{\mathrm{mrc}}$, by substituting (3) into (46) and using [31, eq. (3.381.4), p. 364]

$$\frac{\langle C \rangle_{\mathrm{cifr}}^{\mathrm{mrc}}}{B} = \log_2(1 + (M-1)\overline{\gamma}). \tag{49}$$
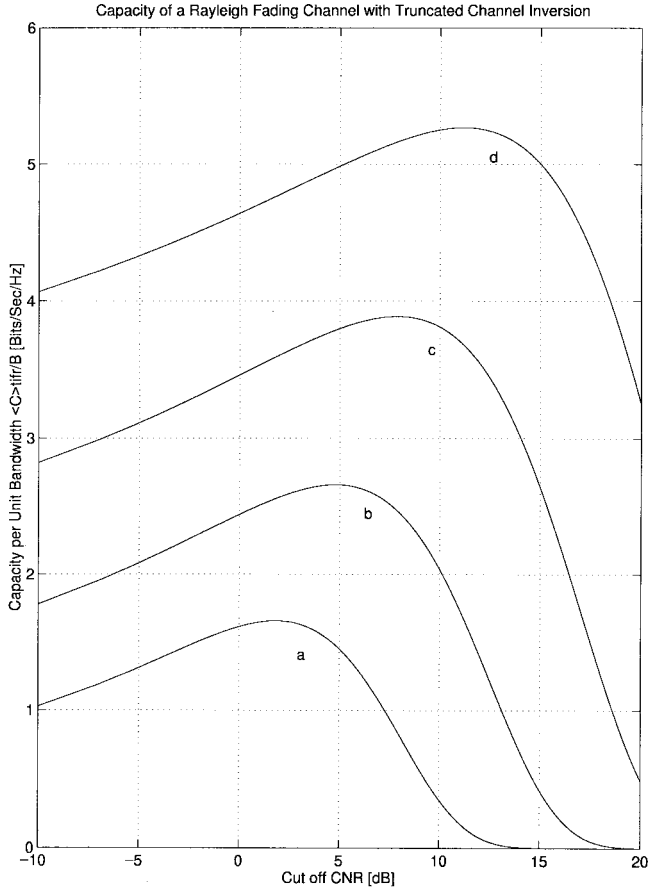
Fig. 2. Channel capacity per unit bandwidth for a Raleigh fading channel versus cutoff CNR γ_o with truncated channel inversion and $\overline{\gamma} =$ (a) 5, (b) 10, (c) 15, and (d) 20 dB.

Fig. 3. Channel capacity per unit bandwidth for a Raleigh fading channel versus cutoff CNR γ_o with truncated channel inversion, MRC diversity ($M = 2$), and $\overline{\gamma} =$ (a) 5, (b) 10, (c) 15, and (d) 20 dB.

Note that the capacity of this policy for a Rayleigh fading channel with an M-branch perfect MRC combiner (49) is the same as the capacity of a set of $M - 1$ parallel independent AWGN channels [35, eq. (15)].

Truncated channel inversion improves the capacity (49) at the expense of outage probability $P_{\text{out}}^{\text{mrc}}$. The capacity of truncated channel inversion with MRC combining, $\langle C \rangle_{\text{tifr}}^{\text{mrc}}$, is obtained by inserting (3) in (47) and using [31, eq. (3.381.3), p. 364]

$$\frac{\langle C \rangle_{\text{tifr}}^{\text{mrc}}}{B} = \log_2 \left(1 + \frac{(M-1)! \overline{\gamma}}{\Gamma(M-1, \gamma_o/\overline{\gamma})} \right) \frac{\Gamma(M, \gamma_o/\overline{\gamma})}{(M-1)!}. \quad (50)$$

Using property (66) of the complementary incomplete gamma function, we can rewrite (50) as the simple expression

$$\frac{\langle C \rangle_{\text{tifr}}^{\text{mrc}}}{B} = \log_2 \left(1 + \frac{(M-1)\overline{\gamma}}{\mathcal{P}_{M-1}(\gamma_o/\overline{\gamma})} \right) \mathcal{P}_M(\gamma_o/\overline{\gamma}), \qquad M \geq 2. \quad (51)$$

Fig. 3 shows the dependence of $\langle C \rangle_{\text{tifr}}^{\text{mrc}}/B$ on γ_o at different $\overline{\gamma}$ values for two-branch MRC diversity. Comparing Figs. 2 and 3 we see that, for a fixed $\overline{\gamma}$, the maximizing cutoff CNR γ_o^* increases when MRC diversity is used. In addition, the relative flatness of the curves in Fig. 3 for $\gamma_o < \gamma_o^*$ indicates that the capacity improvement provided by truncated channel inversion ($\gamma_o = \gamma_o^*$) compared to total channel inversion ($\gamma_o = 0$) is relatively small, and this little improvement comes at the expense of a higher probability of outage (see Fig. 12). This suggests that as long as diversity is used, total channel inversion is a better alternative than truncated channel inversion.

C. Selection Combining

We obtain the capacity per unit bandwidth of a Rayleigh fading channel with total channel inversion and SC diversity, $\langle C \rangle_{\text{cifr}}^{\text{sc}}$, by substituting (5) in (46), as given in (52) at the

$$\frac{\langle C \rangle_{\text{cifr}}^{\text{sc}}}{B} = \log_2 \left(1 + \frac{\overline{\gamma}}{M \lim_{u \to 0^+} \sum_{k=0}^{M-1} (-1)^k \binom{M-1}{k} E_1((1+k)u/\overline{\gamma})} \right). \quad (52)$$
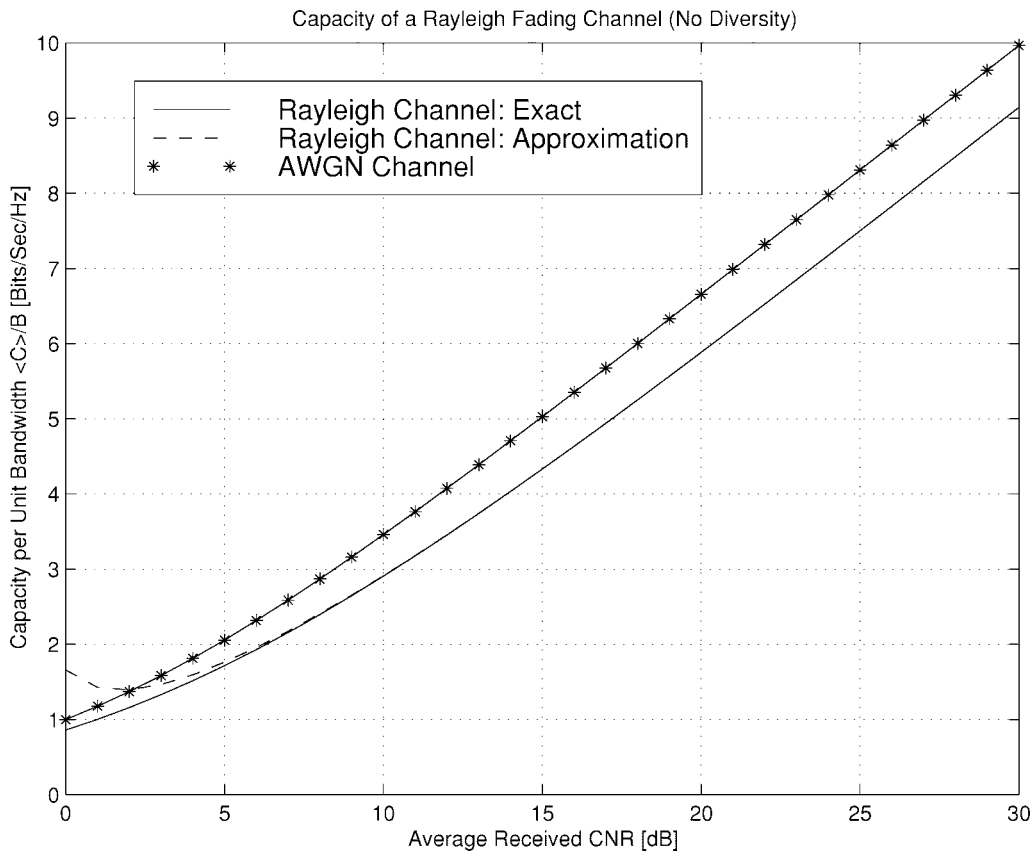
Fig. 4.   Average channel capacity per unit bandwidth for a Raleigh fading and an AWGN channel versus average carrier-to-noise ratio $\overline{\gamma}$ (with no diversity).

bottom of the previous page. When truncated channel inversion is used in combination with SC the capacity per unit bandwidth becomes (53), given at the bottom of the page. Recall that $P_{\text{out}}^{\text{sc}}$ tends to zero as γ_o tends to zero (i.e., total channel inversion). Hence, as expected, we see that (53) reduces to (52) when γ_o tends to zero.

VI. NUMERICAL RESULTS AND COMPARISONS

In this section, we start by comparing the capacity of an AWGN channel (C_{awgn}) with the capacity of a Rayleigh channel with optimal rate adaptation, $\langle C \rangle_{\text{ora}}$, constant transmit power, and various diversity-combining techniques. We then compare the Rayleigh channel capacities for the various adaptation policies and diversity-combining techniques.

A. Comparison with AWGN Channel Capacity

In Fig. 4, channel capacity without diversity, $\langle C \rangle_{\text{ora}}$, given by (34), as well as its asymptotic approximation (36), are plotted against $\overline{\gamma}$. This figure also displays the capacity per

unit bandwidth of an AWGN channel C_{awgn} (30). With these results we find, for example, the following.

- For $\overline{\gamma} = 10$ dB, $\langle C \rangle_{\text{ora}} \simeq 2.91B$, whereas $C_{\text{awgn}} \simeq 3.46B$.
- For $\overline{\gamma} = 25$ dB, $\langle C \rangle_{\text{ora}} \simeq 7.50B$, whereas $C_{\text{awgn}} \simeq 8.31B$.

Therefore, the channel capacity of a Rayleigh fading channel is reduced by 15.9% for $\overline{\gamma} = 10$ dB and by 9.75% for $\overline{\gamma} = 25$ dB.[3] Note in Fig. 4 that the asymptotic approximation (36) closely matches the exact average capacity (34) when $\overline{\gamma} > 5$ dB.

Fig. 5 shows plots of $\langle C \rangle_{\text{ora}}^{\text{mrc}}/B$ (40) as well as its asymptotic approximation (42) as functions of the average CNR *per branch* $\overline{\gamma}$ for $M = 1$, 2, and 4. We use the CNR per branch for this comparison so that we can later compare the improvements provided by MRC and SC diversity schemes on a fair basis, as we will explain in more detail below. Note the

[3] These results correct the 32% and 11% values reported in [28]. Moreover, from Fig. 4, note that a smaller value of $\overline{\gamma}$ results in a smaller difference between C_{awgn} and $\langle C \rangle_{\text{ora}}$, contrary to what was concluded in [28].

$$\frac{\langle C \rangle_{\text{tifr}}^{\text{sc}}}{B} = \log_2 \left(1 + \frac{\overline{\gamma}}{M \sum_{k=0}^{M-1} (-1)^k \binom{M-1}{k} E_1((1+k)\gamma_o/\overline{\gamma})} \right) (1 - P_{\text{out}}^{\text{sc}}). \tag{53}$$
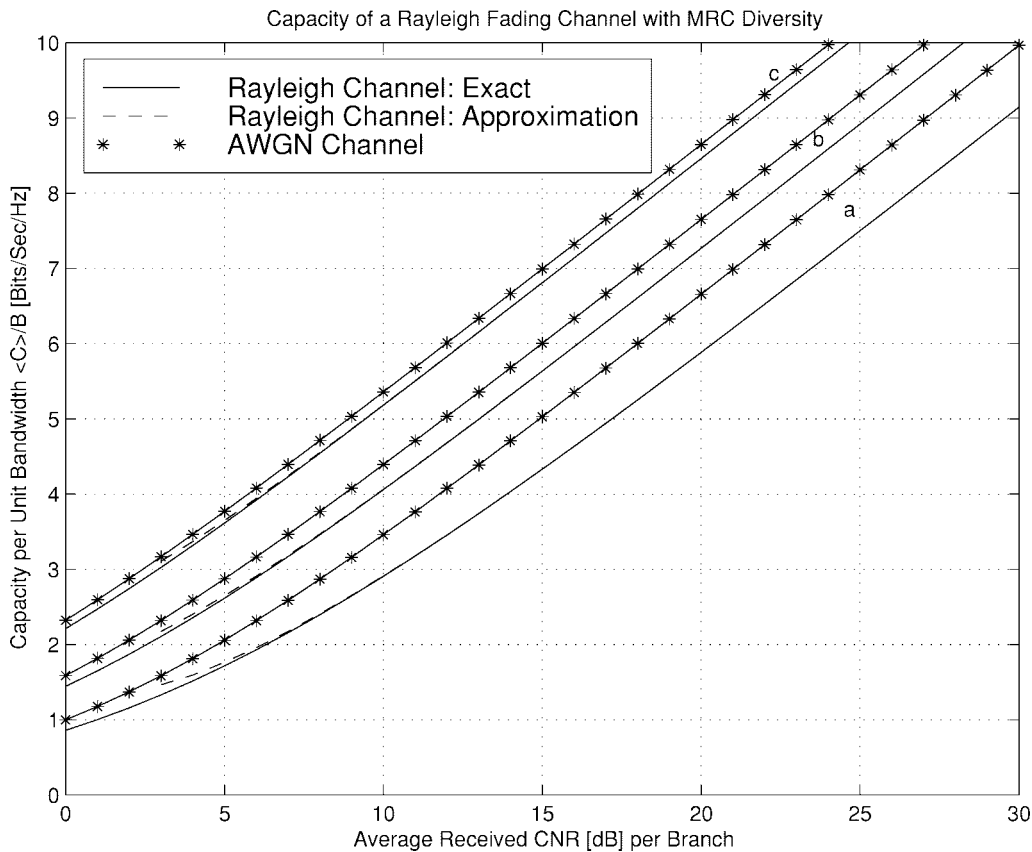
Fig. 5. Average channel capacity per unit bandwidth for a Raleigh fading channel with MRC diversity versus average CNR per branch $\overline{\gamma}$ [(a) $M = 1$, (b) $M = 2$, and (c) $M = 4$].

large diversity gain obtained by two-branch combining: the capacity with two branches in fading exceeds that of a single-branch AWGN channel. Fig. 5 also displays the capacity per unit bandwidth of an array of M-independent AWGN channels with optimal combining (MRC) [35, eq. (15)]

$$\frac{C_{\text{awgn}}^{\text{mrc}}}{B} = \log_2\left(1 + M\gamma\right). \tag{54}$$

Note that the capacity of an array of M-independent Rayleigh channels with MRC combining approaches the capacity of an array of M-independent AWGN channels as M tends to infinity. Note also the diminishing capacity returns that are obtained as the number of branch increases. This diminishing returns characteristic is also exhibited when the performance evaluation is based on outage probabilities [4]. Finally, note again that the asymptotic approximation (42) closely matches the exact average capacity (40) when $\overline{\gamma} > 5$ dB.

Fig. 6 shows plots of $\langle C \rangle_{\text{ora}}^{\text{sc}}/B$ (44) as well as its asymptotic approximation (45) as function of the average CNR per branch $\overline{\gamma}$ for $M = 1$, 2, and 4. Comparing Figs. 5 and 6 we see that, as expected, the SC scheme provides less diversity gain and a lower rate of improvement than the MRC scheme. However, the greatest improvement is still obtained in going from single- to two-branch combining, which again yields a higher capacity than that of a single-branch AWGN channel. Fig. 6 also displays the capacity per unit bandwidth of an array

of M-independent AWGN channels with selection combining

$$\frac{C_{\text{awgn}}^{\text{sc}}}{B} = \log_2\left(1 + \sum_{n=1}^{M} \frac{1}{n}\gamma\right). \tag{55}$$

We again note that the capacity of an array of M-independent Rayleigh channels approaches the capacity of an array of M-independent AWGN channels as M tends to infinity. Finally, for all M the asymptotic approximation (45) closely matches the exact average capacity (44) when $\overline{\gamma} > 5$ dB.

For the M-branch MRC diversity scheme, the average combined CNR $\langle \gamma \rangle_{\text{mrc}}$ is related to the average CNR per branch $\overline{\gamma}$ by [4, eq. (5.2-16), p. 319] $\langle \gamma \rangle_{\text{mrc}} = M\overline{\gamma}$. We can therefore also express $\langle C \rangle_{\text{ora}}^{\text{mrc}}/B$ in terms of $\langle \gamma \rangle_{\text{mrc}}$ as

$$\frac{\langle C \rangle_{\text{ora}}^{\text{mrc}}}{B} = \log_2(e) \exp\left(\frac{M}{\langle \gamma \rangle_{\text{mrc}}}\right) \sum_{k=0}^{M-1} \left(\frac{M}{\langle \gamma \rangle_{\text{mrc}}}\right)^k$$
$$\cdot \Gamma\left(-k, \frac{M}{\langle \gamma \rangle_{\text{mrc}}}\right). \tag{56}$$

Fig. 7 shows plots of $\langle C \rangle_{\text{ora}}^{\text{mrc}}/B$ versus the average combined CNR $\langle \gamma \rangle_{\text{mrc}}$ for $M = 1$, 2, and 4. These plots show the same numerical results as [28, Fig. 2] for $M \geq 2$ and [30, Fig. 1] for $M \geq 1$. These results show that, when expressed in terms of the average combined CNR, the capacity of a Rayleigh channel can never "beat" the capacity of a single-branch AWGN channel, but it comes close to the AWGN channel capacity as the number of diversity branches M approaches infinity.
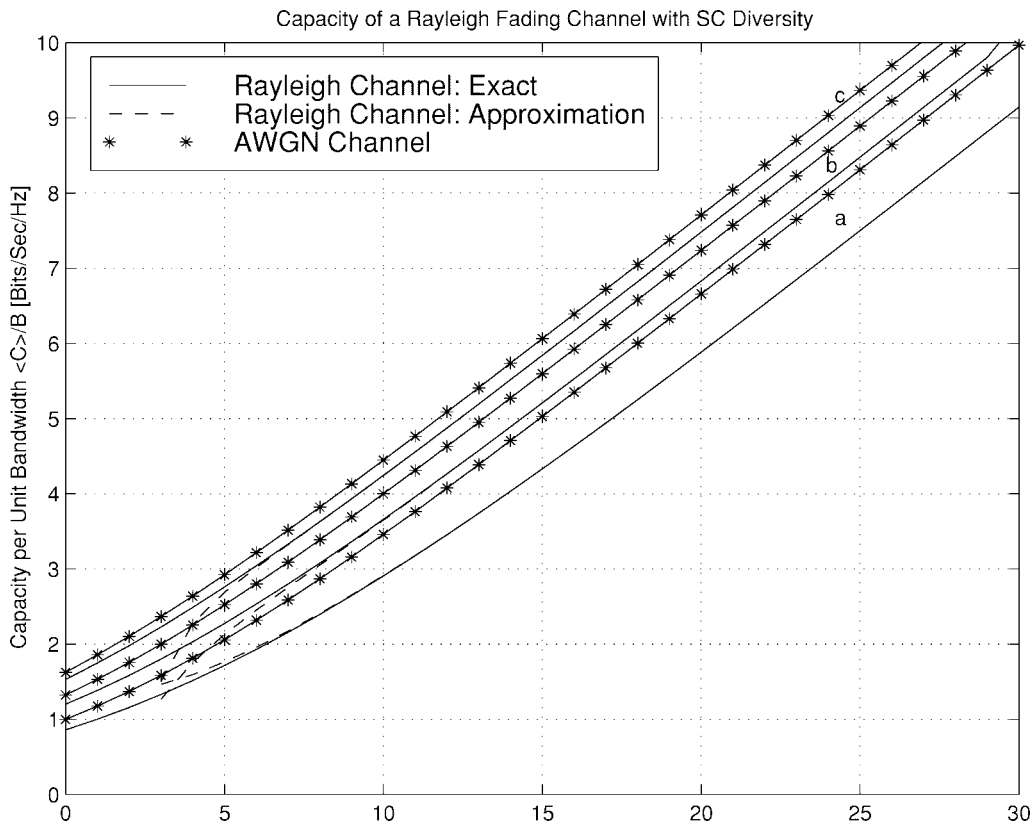
Fig. 6. Average channel capacity per unit bandwidth for Raleigh fading channels with selection-combining diversity versus the average CNR per branch $\overline{\gamma}$ [(a) $M = 1$, (b) $M = 2$, and (c) $M = 4$].
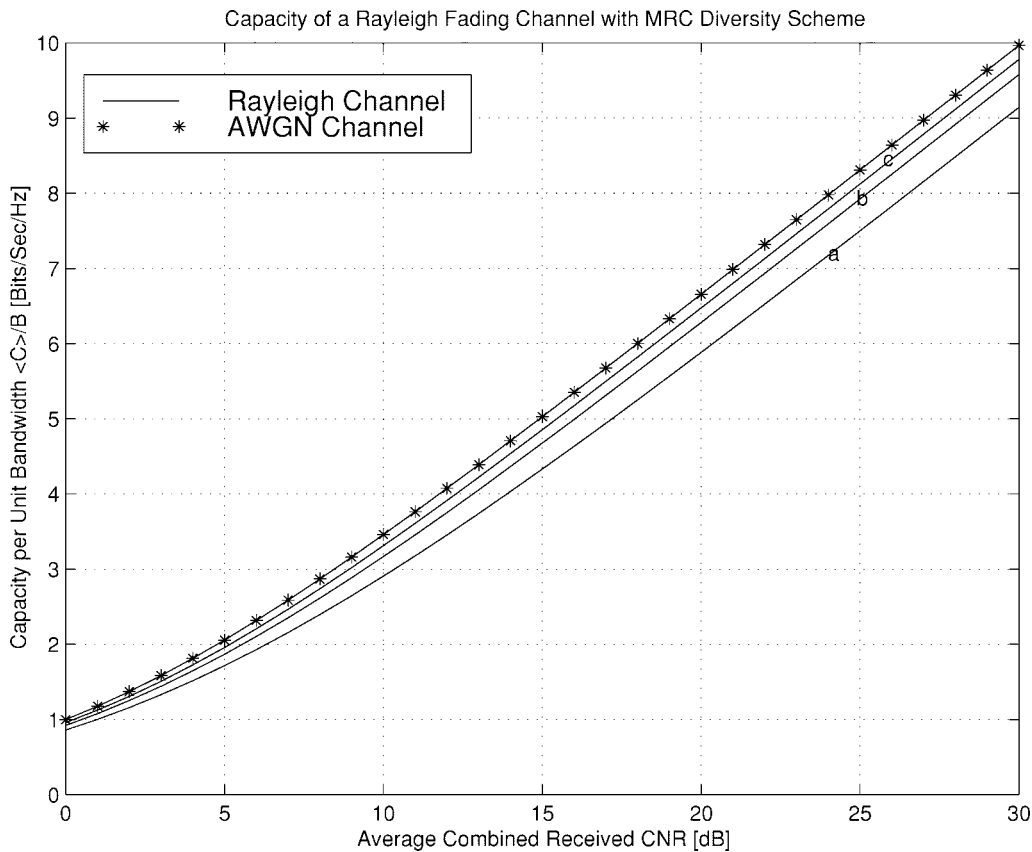
Fig. 7. Average channel capacity per unit bandwidth for a Raleigh fading channel with MRC diversity versus average combined CNR $\langle\gamma\rangle_{\mathrm{mrc}}$ [(a) $M = 1$, (b) $M = 2$, and (c) $M = 4$].
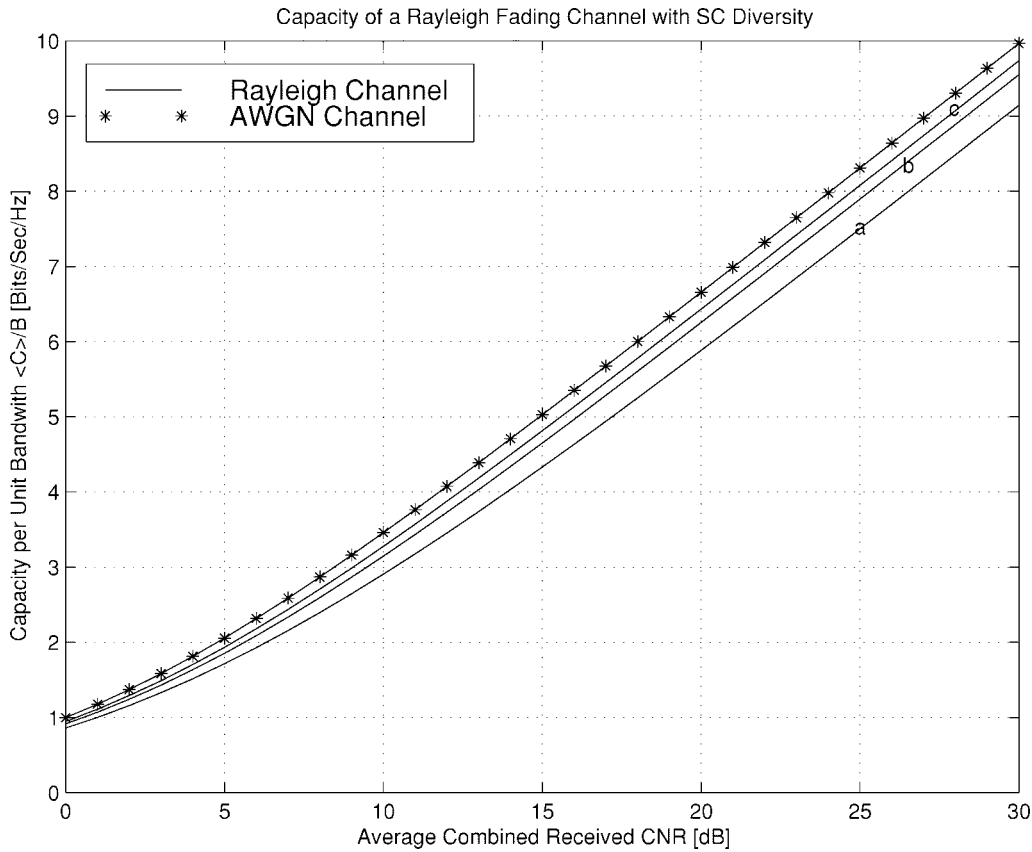
Fig. 8. Average channel capacity per unit bandwidth for Raleigh fading channels with selection combining diversity versus the average combined CNR $\langle\gamma\rangle_{\mathrm{sc}}$ [(a) $M = 1$, (b) $M = 2$, and (c) $M = 4$].

For the M-branch SC diversity scheme, the average combined CNR $\langle\gamma\rangle_{\mathrm{sc}}$ is related to the average CNR of a single branch $\overline{\gamma}$ by [4, eq. (5.2-8), p. 316] $\langle\gamma\rangle_{\mathrm{sc}} = \overline{\gamma}\Sigma_{n=1}^{M}(1/n)$. We can therefore also express $\langle C\rangle_{\mathrm{ora}}^{\mathrm{sc}}/B$ in terms of $\langle\gamma\rangle_{\mathrm{sc}}$ as

$$\frac{\langle C\rangle_{\mathrm{ora}}^{\mathrm{sc}}}{B} = M\log_2(e)\sum_{k=0}^{M-1}\frac{(-1)^k}{1+k}\binom{M-1}{k}$$

$$\cdot\exp\left(\frac{(1+k)\sum_{n=1}^{M}\dfrac{1}{n}}{\langle\gamma\rangle_{\mathrm{sc}}}\right)E_1\left(\frac{(1+k)\sum_{n=1}^{M}\dfrac{1}{n}}{\langle\gamma\rangle_{\mathrm{sc}}}\right).$$

(57)

Fig. 8 shows plots of $\langle C\rangle_{\mathrm{ora}}^{\mathrm{sc}}/B$ versus the average combined CNR $\langle\gamma\rangle_{\mathrm{sc}}$ for $M = 1$, 2, and 4. In fact, Figs. 7 and 8 are very similar, since $\langle C\rangle_{\mathrm{ora}}^{\mathrm{sc}}$ approaches the capacity of the single-branch AWGN channel C as the number of diversity branches M increases. However, a close look at the numerical results shows that for a fixed M, $\langle C\rangle_{\mathrm{ora}}^{\mathrm{mrc}}$ is always slightly bigger than $\langle C\rangle_{\mathrm{ora}}^{\mathrm{sc}}$ for an equal average CNR at the output of the combiner (i.e., for $\langle\gamma\rangle_{\mathrm{mrc}} = \langle\gamma\rangle_{\mathrm{sc}}$). Note that this slim differences is due to the fact that the average CNR per branch for SC $(\overline{\gamma} = \langle\gamma\rangle_{\mathrm{sc}}/\Sigma_{n=1}^{M}(1/n))$ is bigger than the average CNR per branch for MRC $(\overline{\gamma} = \langle\gamma\rangle_{\mathrm{mrc}}/M)$ for an equal average combined CNR. That is why, as mentioned above, we believe that a fair comparison between the MRC and SC diversity schemes should be based on the average CNR per

branch (Figs. 5 and 6). However, when looked at individually, Figs. 7 and 8 are also of interest since they show that the capacity of a single-branch AWGN channel with CNR $\overline{\gamma}$ is always bigger than the capacity of a fading channel with the same average received CNR $\overline{\gamma}$ at the output of the diversity combiner, regardless of the adaptation and diversity-combining strategy in the latter case.

B. Comparison of the Different Policies

Fig. 9 shows the calculated channel capacity per unit bandwidth as a function of $\overline{\gamma}$ for the different adaptation policies without diversity combining. These curves confirm the previous numerical results reported in [27] using the closed-form expressions (17), (34), and (48) instead of numerical integration. From this figure, we see that the optimal power and rate adaptation (17) yields a small increase in capacity over just rate adaptation (34), and this small increase in capacity diminishes as $\overline{\gamma}$ increases. The corresponding outage probability (18) for the optimal adaptation and truncated channel inversion (with optimal cutoff γ_o^*) are shown in Fig. 10.

Fig. 11 shows the channel capacity per unit bandwidth as a function of $\overline{\gamma}$ for the different policies with MRC diversity for $M = 1$, 2, and 4. As the number of combining branches increases the capacity difference between optimal power and rate adaptation versus optimal rate adaptation alone becomes negligible for all values of $\overline{\gamma}$. For any M, fixed rate
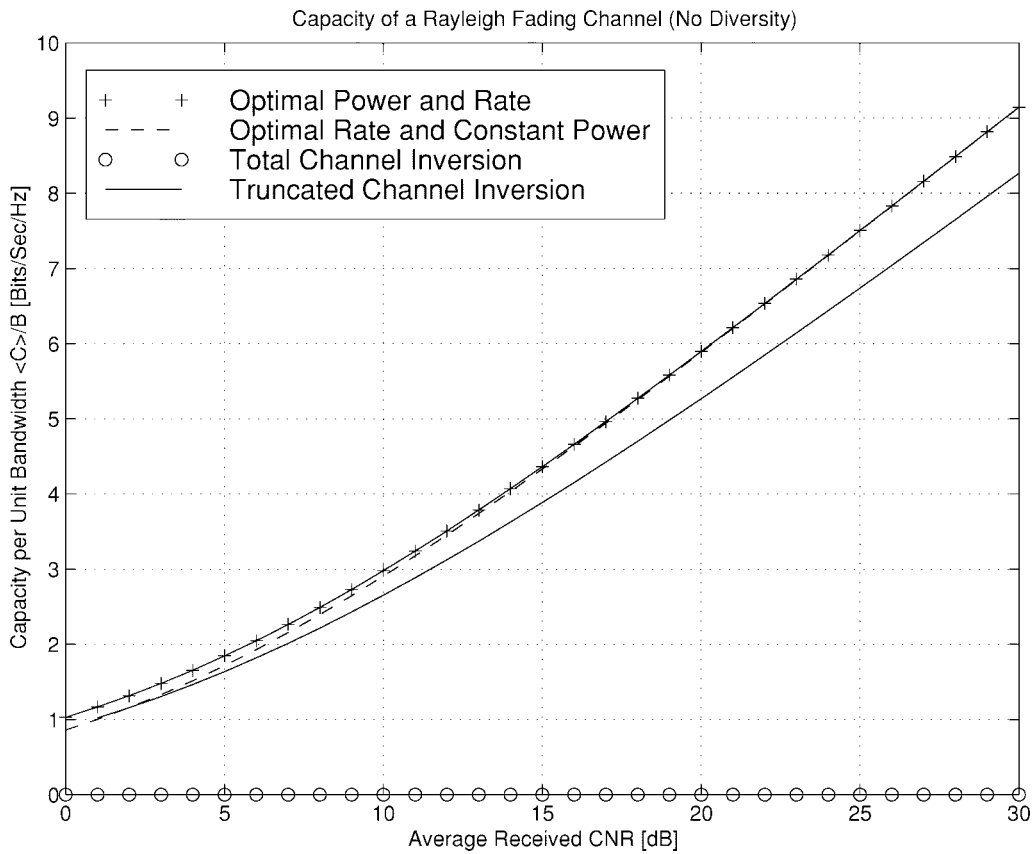
Fig. 9. Channel capacity per unit bandwidth for a Raleigh fading channel versus average carrier-to-noise ratio $\bar{\gamma}$ for different adaptation policies with no diversity.
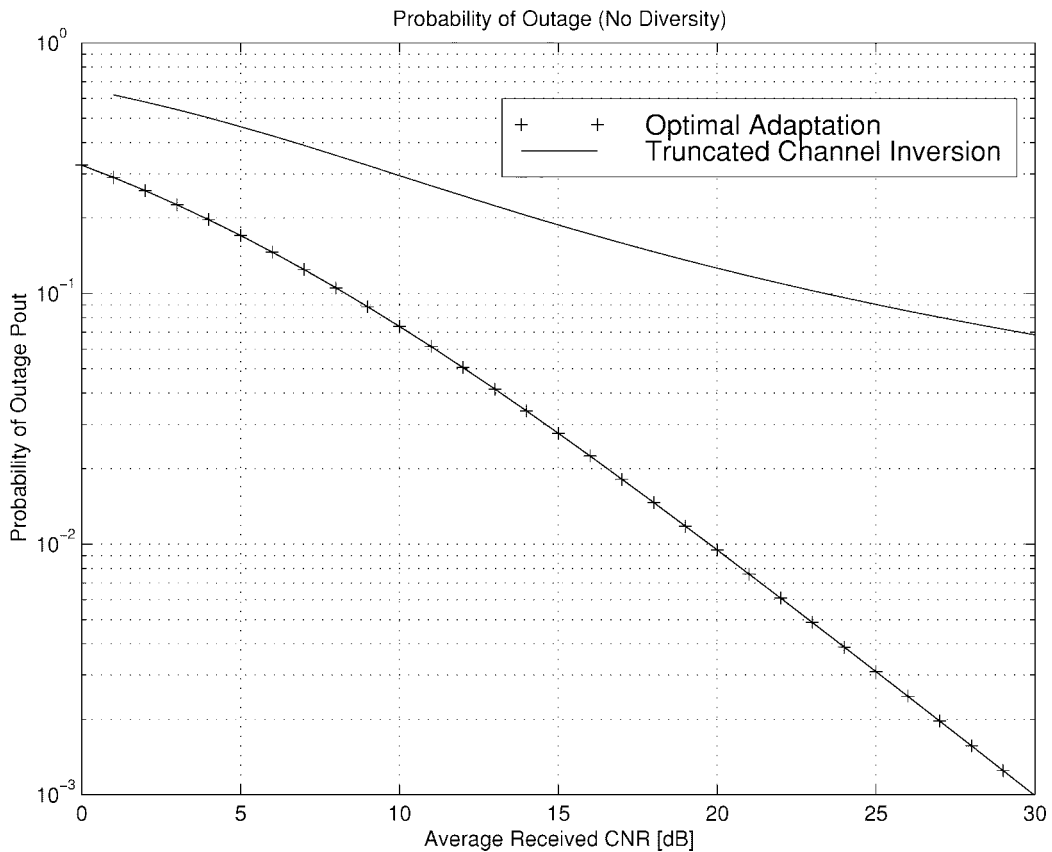
Fig. 10. Outage probability of the optimal adaptation and truncated channel inversion.
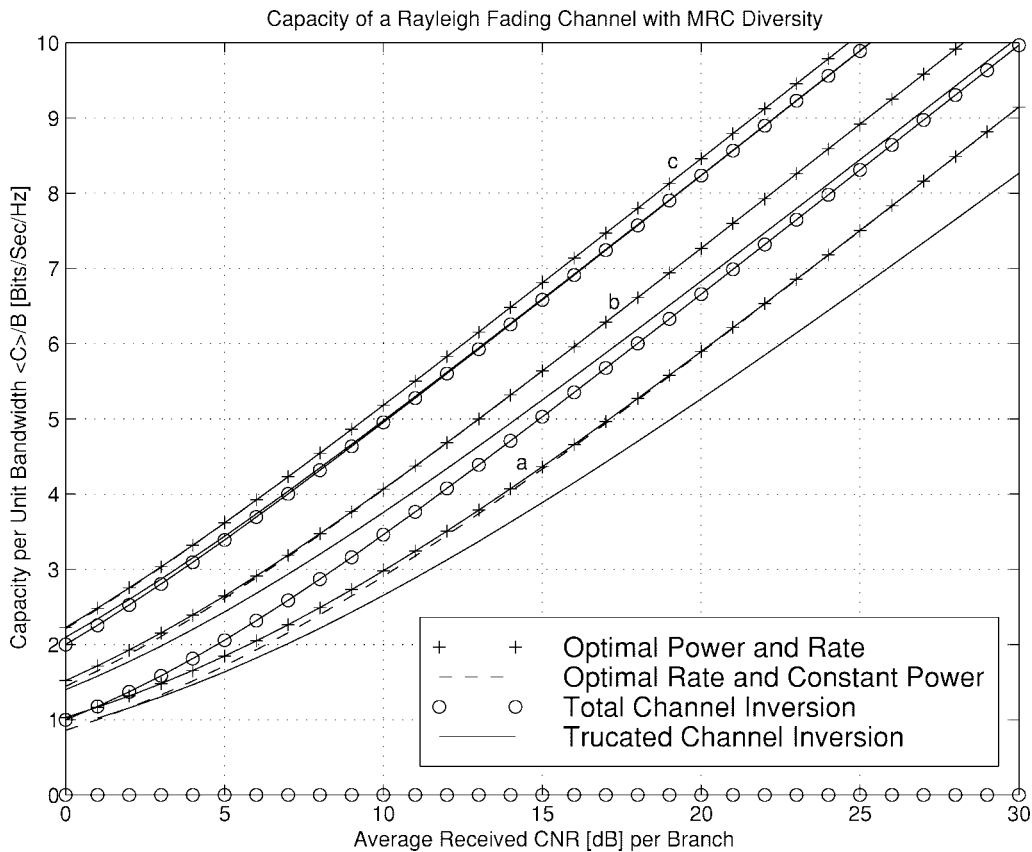
Fig. 11. Channel capacity per unit bandwidth for a Raleigh fading channel versus average carrier-to-noise ratio $\overline{\gamma}$ for different adaptation policies with MRC diversity [(a) $M = 1$, (b) $M = 2$, and (c) $M = 4$].

transmission with total channel inversion suffers the largest capacity penalty relative to the other policies. However, as M increases, the fading is progressively reduced, and this penalty diminishes remarkably. Thus, as M increases, all capacities of the various policies converge to the capacity of an array of M-independent AWGN channels (54). However, it is not possible in practice to completely eliminate the effects of fading through space diversity since the number of diversity branches is limited. This is especially true for the downlink (base station to mobile), since mobile receivers are generally constrained in size and power.

Since channel inversion is the least complex technique, there is a tradeoff of complexity and capacity for the various adaptation methods and diversity-combining techniques. The diversity gain for all policies is quite important, especially for total channel inversion. For example, in Fig. 11 we see that the capacity with total channel inversion and two-branch MRC exceeds that of a single-branch system with optimal adaptation. Note that this figure also illustrates the typical diminishing returns obtained as the number of branches increases. In addition, for $M = 1$ total channel inversion suffers a large capacity penalty relative to truncated channel inversion. However, as the number of combining branches M increases, the effect of fading is progressively reduced, and this penalty diminishes remarkably. In particular, as M increases, we see that truncated channel inversion yields a small increase in capacity over total channel inversion, and this small increase in capacity diminishes as the average CNR $\overline{\gamma}$ and/or the number

of combined branches M increase. The corresponding outage probability (23) for the optimal adaptation and truncated channel inversion (with optimal cutoff γ_o^*) policies with MRC are shown in Fig. 12.

Fig. 13 shows the channel capacity per unit bandwidth as a function of $\overline{\gamma}$ for the different adaptation policies with SC diversity for $M = 1$, 2, and 4. As expected, SC provides less diversity gain than MRC, with rapidly diminishing returns as M increases. However, the diversity impact on channel inversion is still important for SC diversity, since the capacity with this policy and with two-branch combining exceeds that of a single-branch system with optimal adaptation for all $\overline{\gamma} > 8$ dB.

Fig. 14 compares the channel capacity per unit bandwidth as function of $\overline{\gamma}$ for the different adaptation policies with: 1) four-branch MRC diversity and 2) four-branch SC diversity. These curves illustrate the extra diversity gain provided by MRC over SC. We see from this figure that MRC provides about 1-b/s/Hz improvement over SC at any $\overline{\gamma}$ and for any of the considered adaptive transmission policies.

VII. CONCLUSION

We have examined the Shannon capacity or, equivalently, the upper-bound on spectral efficiency of three adaptive transmission techniques over Rayleigh fading channels. In particular, we obtained closed-form expressions for the capacity when
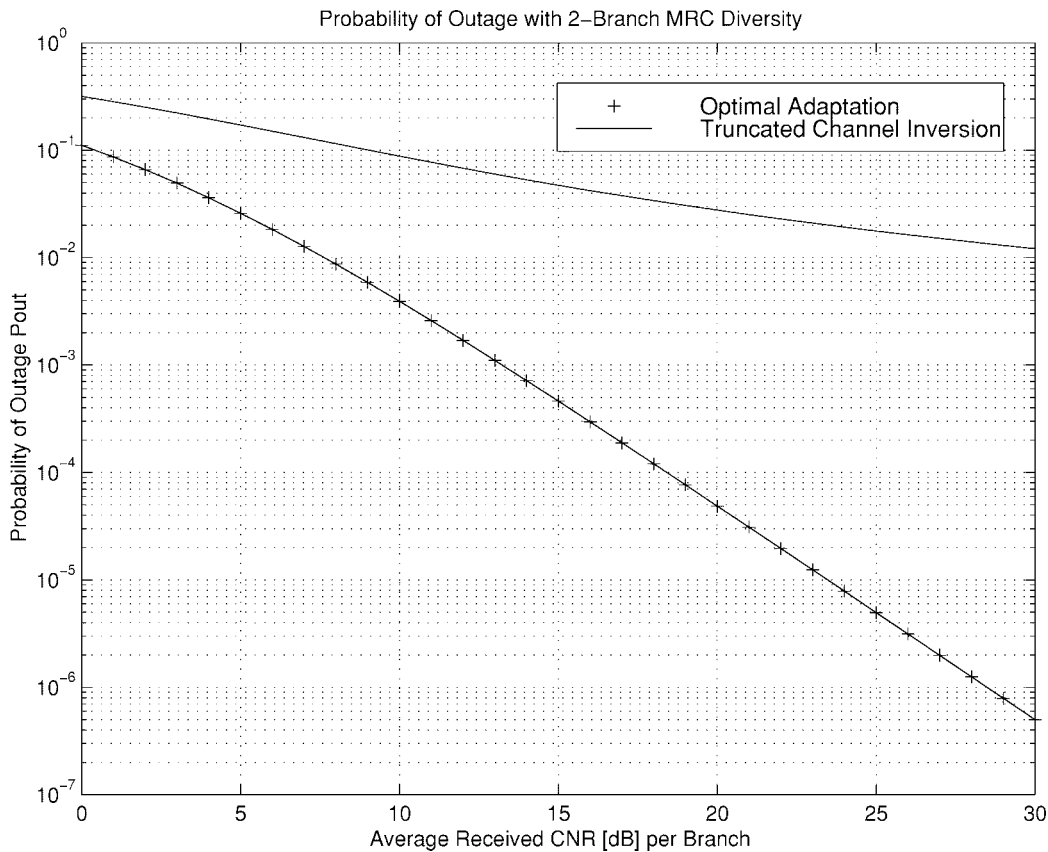
Fig. 12. Outage probability of the optimal adaptation and truncated channel inversion with MRC diversity.

these adaptive schemes are used in conjunction with diversity combining.

We first compared the capacity of an AWGN channel with the capacity of a Rayleigh channel with optimal rate adaptation and constant transmit power. When expressed in terms of the average CNR per branch, the capacity of an array of M-independent Rayleigh channels is bigger than the capacity of a single-branch AWGN channel, but is always smaller than the capacity of an array of M-independent AWGN channels and converges to it as M tends to infinity. On the other hand, when expressed in terms of the average combined CNR, the capacity of a Rayleigh channel with diversity cannot "beat" the capacity of a single-branch AWGN channel, but comes close to it as the number of diversity branches approaches infinity.

We also compared the channel capacities of the various adaptation policies both with and without diversity combining. Optimal power and rate adaptation yields a small increase in capacity over just optimal rate adaptation, and this small increase in capacity diminishes as the average received CNR and/or the number of diversity branches increases. In addition, channel inversion suffers the largest capacity penalty relative to the two other policies. However, this capacity penalty diminishes and all capacities approach the capacity of the AWGN channel with increasing diversity.

Diversity yields large capacity gains for all the techniques with diminishing returns on the number of branches. The diversity gain is most pronounced for channel inversion. In addition, selection combining provides less diversity gain than MRC for all the adaptive policies, as expected.

Although the results derived herein are Shannon bounds, similar analysis has been applied to adaptive MQAM modulation without diversity [21]. Thus, we expect that the same general trends will be observed on any adaptive modulation method, although the spectral efficiency will be smaller.

APPENDIX A
EVALUATION OF $\mathcal{J}_n(\mu)$ (14)

We evaluate the integral $\mathcal{J}_n(\mu)$ defined in (14) using partial integration, namely

$$\int_1^{+\infty} u \, dv = \lim_{t \to +\infty} (uv) - \lim_{t \to 1} (uv) - \int_1^{+\infty} v \, du. \quad (58)$$

First, let

$$u = \ln t. \quad (59)$$

Thus

$$du = \frac{dt}{t}. \quad (60)$$

Then, let

$$dv = t^{n-1} e^{-\mu t} \, dt. \quad (61)$$

Performing $n-1$ successive integration by parts yields [31, eq. (2.321.2), p. 112]

$$v = -e^{-\mu t} \sum_{k=1}^{n} \frac{(n-1)!}{(n-k)!} \frac{t^{n-k}}{\mu^k}. \quad (62)$$
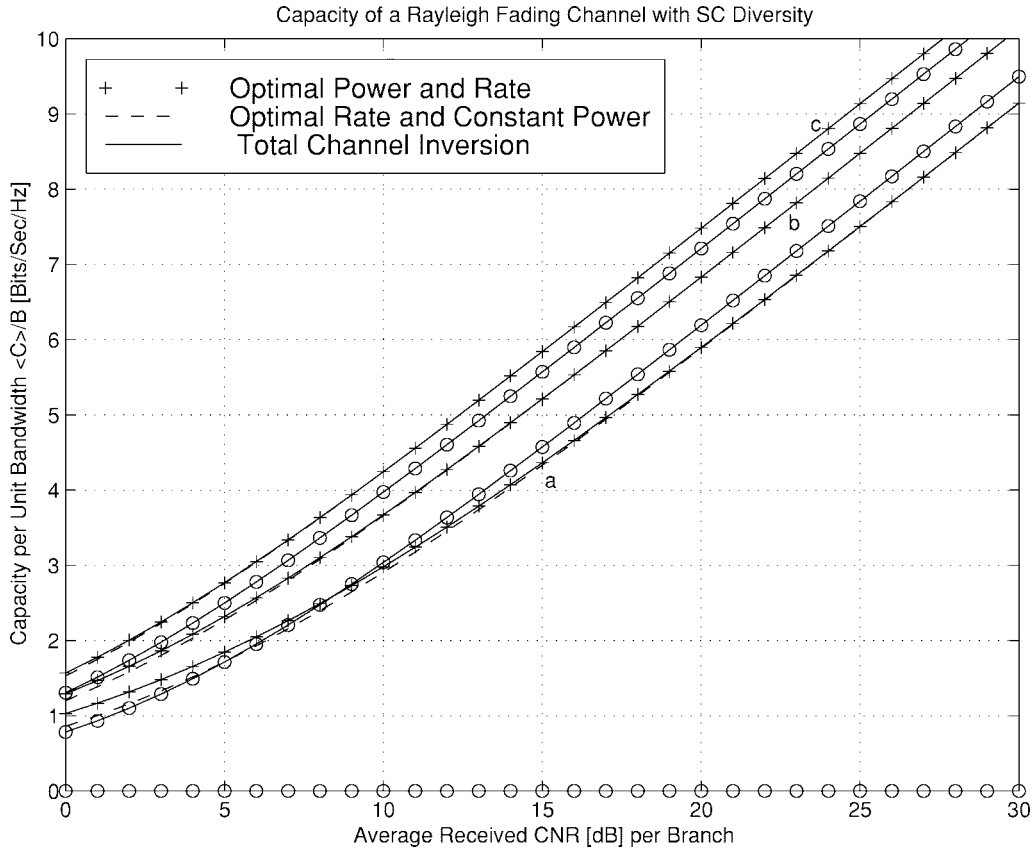
Fig. 13. Channel capacity per unit bandwidth for a Raleigh fading channel versus average carrier-to-noise ratio $\overline{\gamma}$ for different adaptation policies with SC diversity [(a) $M = 1$, (b) $M = 2$, and (c) $M = 4$].

Substituting (59), (62), and (60) in (58), we see that the first two terms go to zero. Hence

$$\mathcal{J}_n(\mu) = \sum_{k=1}^{n} \frac{(n-1)!}{\mu^k (n-k)!} \int_1^{+\infty} t^{n-k-1} e^{-\mu t} \, dt. \qquad (63)$$

The integral in (63) can be written in a closed form with the help of [31, eq. (3.381.3), p. 364], giving

$$\mathcal{J}_n(\mu) = \frac{(n-1)!}{\mu^n} \sum_{k=0}^{n-1} \frac{\Gamma(k,\mu)}{k!} \qquad (64)$$

where $\Gamma(\cdot, \cdot)$ is the complementary incomplete gamma function (or Prym's function as it is sometimes called) defined by [31, eq. (8.350.2), p. 949]

$$\Gamma(\alpha, x) = \int_x^{+\infty} t^{\alpha-1} e^{-t} \, dt. \qquad (65)$$

For k positive integers

$$\Gamma(k, \mu) = (k-1)! \mathcal{P}_k(\mu), \qquad k \geq 2 \qquad (66)$$

where $\mathcal{P}_k(\cdot)$ denotes the Poisson distribution defined as

$$\mathcal{P}_k(\mu) = e^{-\mu} \sum_{j=0}^{k-1} \frac{\mu^j}{j!}. \qquad (67)$$

For $k = 0$ [31, eq. (8.359.1) p. 951]

$$\Gamma(0, \mu) = E_1(\mu) \qquad (68)$$

where $E_1(\cdot)$ is the exponential integral of first-order function defined as

$$E_1(x) = \int_1^{+\infty} \frac{e^{-xt}}{t} \, dt. \qquad (69)$$

Thus, for n positive integers, (64) can be written as

$$\mathcal{J}_n(\mu) = \frac{(n-1)!}{\mu^n} \left(E_1(\mu) + \sum_{k=1}^{n-1} \frac{\mathcal{P}_k(\mu)}{k} \right). \qquad (70)$$

In particular, when $n = 1$, (70) reduces to

$$\mathcal{J}_1(\mu) = \frac{E_1(\mu)}{\mu}. \qquad (71)$$

APPENDIX B
EVALUATION OF $\mathcal{I}_n(\mu)$ (32)

We evaluate the integral $\mathcal{I}_n(\mu)$ defined in (32) using partial integration, namely

$$\int_0^{+\infty} u \, dv = \lim_{t \to +\infty} (uv) - \lim_{t \to 0} (uv) - \int_0^{+\infty} v \, du. \qquad (72)$$

First, let

$$u = \ln(1+t). \qquad (73)$$

Thus

$$du = \frac{dt}{1+t}. \qquad (74)$$
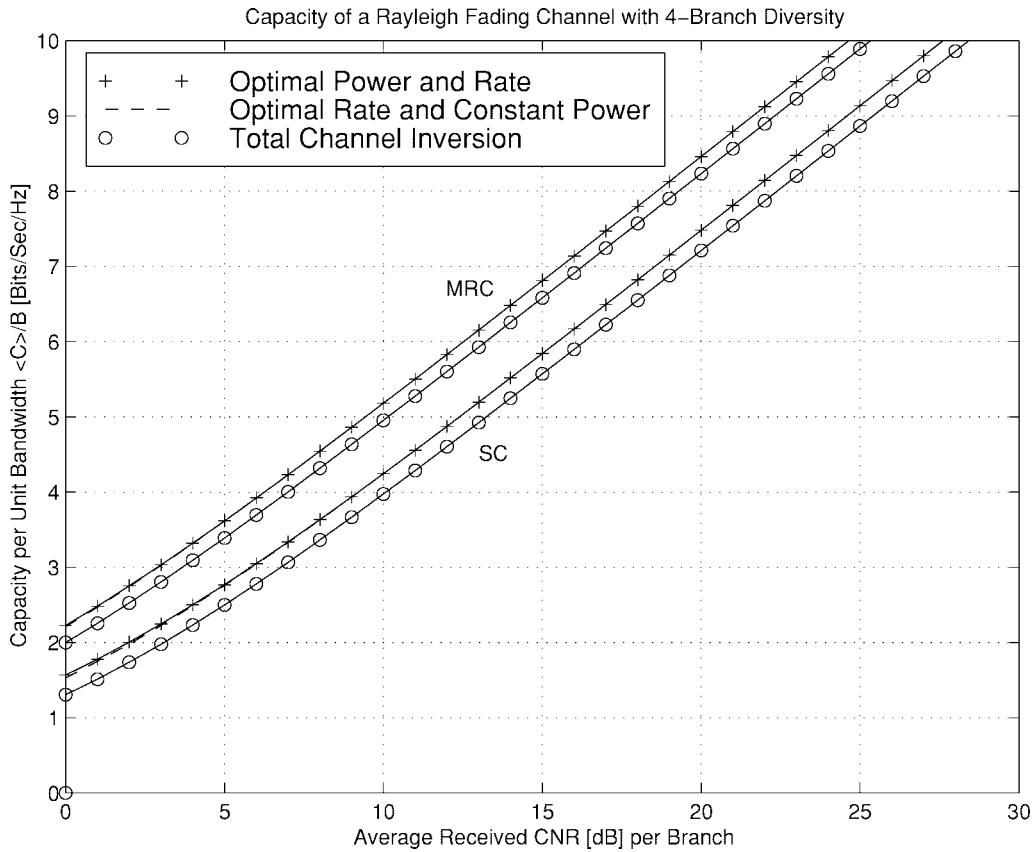
Fig. 14. Channel capacity per unit bandwidth for a Raleigh fading channel versus average carrier-to-noise ratio $\overline{\gamma}$ for different adaptation policies with (a) four-branch MRC diversity combining and (b) four-branch SC diversity combining.

Then, let

$$dv = t^{n-1} e^{-\mu t} \, dt. \qquad (75)$$

Performing $n-1$ successive integration by parts yields [31, eq. (2.321.2), p. 112]

$$v = -e^{-\mu t} \sum_{k=1}^{n} \frac{(n-1)!}{(n-k)!} \frac{t^{n-k}}{\mu^k}. \qquad (76)$$

Substituting (73), (76), and (74) in (72), we see that the first two terms go to zero. Hence

$$\mathcal{I}_n(\mu) = \sum_{k=1}^{n} \frac{(n-1)!}{\mu^k (n-k)!} \int_{0}^{+\infty} \frac{t^{n-k} e^{-\mu t}}{1+t} \, dt. \qquad (77)$$

The integral in (77) can be written in a closed form with the help of [31, eq. (3.383.10), p. 366], giving

$$\mathcal{I}_n(\mu) = (n-1)! e^{\mu} \sum_{k=1}^{n} \frac{\Gamma(-n+k, \mu)}{\mu^k} \qquad (78)$$

where $\Gamma(\cdot, \cdot)$ is the complementary incomplete gamma function defined in (65). Note that when $n = 1$, (78) reduces to

$$\mathcal{I}_1(\mu) = e^{\mu} \frac{\Gamma(0, \mu)}{\mu} \qquad (79)$$

which can be written as

$$\mathcal{I}_1(\mu) = e^{\mu} \frac{E_1(\mu)}{\mu} \qquad (80)$$

where $E_1(\cdot)$ is the exponential integral of first order defined by (69).

REFERENCES

[1] K. Pahlavan and A. H. Levesque, "Wireless data communications," *Proc. IEEE*, vol. 82, pp. 1398–1430, Sept. 1994.
[2] G. L. Stüber, *Principles of Mobile Communications.* Norwell, MA: Kluwer, 1996.
[3] W. T. Webb and L. Hanzo, *Modern Quadrature Amplitude Modulation.* New York: IEEE Press, 1994.
[4] W. C. Jakes, *Microwave Mobile Communication*, 2nd ed. Piscataway, NJ: IEEE Press, 1994.
[5] S. Sampei and T. Sunaga, "Rayleigh fading compensation for QAM in land mobile radio communications," *IEEE Trans. Veh. Technol.*, vol. 42, pp. 137–147, May 1993.
[6] D. Brennan, "Linear diversity combining techniques," in *Proc. IRE*, vol. 47, June 1959, pp. 1075–1102.
[7] T. Sunaga and S. Sampei, "Performance of multi-level QAM with post-detection maximal ratio combining space diversity for digital land-mobile radio communications," *IEEE Trans. Veh. Technol.*, vol. 42, pp. 294–301, Aug. 1993.
[8] S. Sampei, Y. Kamio, and H. Sasaoka, "Field experiments on pilot symbol aided 16 QAM modems for land mobile communications," *Electron. Lett.*, vol. 28, pp. 2198–2199, Dec. 1992.
[9] S. Sampei, E. Moriyama, H. Sasaoka, N. Kinoshita, K. Hiramatsu, K. Inogai, and K. Honma, "Field experiments on a 16 QAM/TDMA system

for land mobile communications," *Electron. Lett.*, vol. 30, pp. 185–186, Feb. 1994.

[10] J. F. Hayes, "Adaptive feedback communications," *IEEE Trans. Commun. Technol.*, vol. COM-16, pp. 29–34, Feb. 1968.

[11] J. K. Cavers, "Variable-rate transmission for Rayleigh fading channels," *IEEE Trans. Commun.*, vol. COM-20, pp. 15–22, Feb. 1972.

[12] V. O. Hentinen, "Error performance for adaptive transmission on fading channels," *IEEE Trans. Commun.*, vol. COM-22, pp. 1331–1337, Sept. 1974.

[13] S. Otsuki, S. Sampei, and N. Morinaga, "Square-QAM adaptive modulation/TDMA/TDD systems using modulation level estimation with Walsh function," *Electron. Lett.*, vol. 31, pp. 169–171, Feb. 1995.

[14] W. T. Webb and R. Steele, "Variable rate QAM for mobile radio," *IEEE Trans. Commun.*, vol. 43, pp. 2223–2230, July 1995.

[15] Y. Kamio, S. Sampei, H. Sasaoka, and N. Morinaga, "Performance of modulation-level-controlled adaptive-modulation under limited transmission delay time for land mobile communications," in *Proc. IEEE Veh. Technol. Conf. VTC'95*, Chicago, IL, July 1995, pp. 221–225.

[16] B. Vucetic, "An adaptive coding scheme for time-varying channels," *IEEE Trans. Commun.*, vol. 39, pp. 653–663, May 1991.

[17] A. Goldsmith and P. Varaiya, "Increasing spectral efficiency through power control," in *Proc. IEEE Int. Conf. Commun. ICC'93*, Geneva, Switzerland, May 1993, pp. 600–604.

[18] S. M. Alamouti and S. Kallel, "Adaptive trellis-coded multiple-phased-shift keying for Rayleigh fading channels," *IEEE Trans. Commun.*, vol. 42, pp. 2305–2314, June 1994.

[19] A. Goldsmith, "Variable-rate coded M-QAM for fading channels," in *Proc. Communication Theory Mini-Conf. (CTMC-III) in Conjunction with IEEE Global Commun. Conf. GLOBECOM'94*, San Francisco, CA, Nov. 1994, pp. 186–190.

[20] T. Ue, S. Sampei, and N. Morinaga, "Symbol rate and modulation level controlled adaptive modulation/TDMA/TDD for personal communication systems," *IEICE Trans. Commun.*, vol. E78-B, pp. 1117–1124, Aug. 1995.

[21] A. J. Goldsmith and S. G. Chua, "Variable-rate variable-power M-QAM for fading channels," *IEEE Trans. Commun.*, vol. 45, pp. 1218–1230, Oct. 1997.

[22] H. Matsuoka, S. Sampei, N. Morinaga, and Y. Kamio, "Symbol rate and modulation level controlled adaptive modulation/TDMA/TDD for personal communication systems," *IEICE Trans. Commun.*, vol. E79-B, pp. 328–334, Mar. 1996.

[23] S. Sampei, N. Morinaga, and Y. Kamio, "Adaptive modulation/TDMA with a BDDFE for 2 Mbit/s multi-media wireless communication systems," in *Proc. IEEE Veh. Technol. Conf. VTC'95*, Chicago, IL, July 1995, pp. 311–315.

[24] G. R. Sugar, "Some fading characteristics of regular VHF ionospheric propagation," in *Proc. IRE*, Oct. 1955, pp. 1432–1436.

[25] K. Bullington, W. J. Inkster, and A. L. Durkee, "Some tropospheric scatter propagation measurements near the radio-horizon," in *Proc. IRE*, Oct. 1955, pp. 1336–1340.

[26] M.-S. Alouini and A. Goldsmith, "Capacity of Nakagami multipath fading channels," in *Proc. IEEE Veh. Technol. Conf. VTC'97*, Phoenix, AZ, May 1997, pp. 358–362.

[27] A. Goldsmith and P. Varaiya, "Capacity of fading channels with channel side information," *IEEE Trans. Inform. Theory*, vol. 43, pp. 1896–1992, Nov. 1997.

[28] W. C. Y. Lee, "Estimate of channel capacity in Rayleigh fading environment," *IEEE Trans. Veh. Technol.*, vol. 39, pp. 187–190, Aug. 1990.

[29] L. Ozarow, S. Shamai, and A. Wyner, "Information theoretic considerations for cellular mobile radio," *IEEE Trans. Veh. Technol.*, vol. 43, pp. 359–378, May 1994.

[30] C. G. Günther, "Comment on "Estimate of channel capacity in Rayleigh fading environment," *IEEE Trans. Veh. Technol.*, vol. 45, pp. 401–403, May 1996.

[31] I. S. Gradshteyn and I. M. Ryzhik, *Table of Integrals, Series, and Products*. San Diego, CA: Academic, 5th ed., 1994.

[32] J. Wolfowitz, *Coding Theorems of Information Theory*, 2nd ed. New York: Springer-Verlag, 1964, Theorem 4.6.1.

[33] T. Ericson, "A Gaussian channel with slow fading," *IEEE Trans. Inform. Theory*, vol. IT-16, pp. 353–355, May 1970.

[34] R. J. McEliece and W. E. Stark, "Channels with block interference," *IEEE Trans. Inform. Theory*, vol. IT-30, pp. 44–53, Jan. 1984.

[35] K. M. Cheung and V. Vilnrotter, "Channel capacity of an array system for Gaussian channels with applications to combining and noise cancellation," JPL/Telecommunications and Data Acquisition Progress Rep. 42-124, Feb. 1996, pp. 53–62.

Mohamed-Slim Alouini (S'94–M'99), for a photograph and biography, see this issue, p. 1066.

Andrea J. Goldsmith (S'94–M'95), for a photograph and biography, see this issue, p. 1066.